Journal of Power Sources 195 (2010) 185–189

Contents lists available at ScienceDirect

Journal of Power Sources

journal homepage: www.elsevier.com/locate/jpowsour

Short communication

Investigation of PtNi/C anode electrocatalysts for direct borohydride fuel cell

Guang-jin Wang, Yun-zhi Gao*, Zhen-bo Wang, Chun-yu Du, Jia-jun Wang, Ge-ping Yin*

School of Chemical Engineering and Technology, Harbin Institute of Technology, Harbin 150001, P.R. China

ARTICLE INFO

Article history:
Received 21 May 2009
Received in revised form 23 June 2009
Accepted 24 June 2009
Available online 2 July 2009

Keywords:
Direct borohydride fuel cell
PtNi/C catalyst
Borohydride electrooxidation
Alloy formation

ABSTRACT

In this study, carbon-supported PtNi alloys with different molar ratios synthesized by borohydride reduction were evaluated as anode catalysts for sodium borohydride fuel cells. The higher angle shifts of the Pt peaks from X-ray diffraction (XRD) account for the alloy formation between Pt and Ni. The negative shift of Pt 4f XPS spectrum for PtNi(7:3)/C also indicates an electronic structural change of Pt in the alloyed PtNi/C catalyst. The cyclic voltammetry (CV) results show that the PtNi(x:10 − x)/C catalysts are electrochemically active toward borohydride oxidation at the potential range between −0.6 V and +0.1 V vs. Hg/HgO electrode, and PtNi(7:3)/C presents the strongest peak current density among three catalysts with different molar ratios. The results of amperometric i–t curves (i–t) tests also show that the steady-state current density is the highest on PtNi(7:3)/C among alloy catalysts. The higher electrocatalytic activity of the PtNi(7:3)/C can be attributed to the alloy effect and the Pt electronic structure change due to the addition of Ni.

1. Introduction

Fuel cells have received increasing attention because of their high efficiency and low pollution in the past decades. Unfortunately, some kinds of fuel cells, such as the proton exchange membrane fuel cell requiring gaseous hydrogen as the fuel, afford a relatively low energy density. Direct borohydride fuel cell (DBFC), as a direct liquid fuel cell with high energy density, i.e. 9296 Wh kg^{-1} for $NaBH_4$, is attracting more interest recently [1,2]. In fact, a DBFC was first proposed in the early 1960s by Indig, Snyder [3], and Jasinski [4]. The electrochemical reactions in a DBFC employing oxygen as oxidant are as follows:

$$\text{Anode}: \ BH_4^- + 8OH^- \rightarrow BO_2^- + 6H_2O + 8e^-, \quad E^0 = -1.24\,\text{V vs. SHE} \tag{1}$$

$$\text{Cathode}: \ 2O_2 + 4H_2O + 8e^- \rightarrow 8OH^-, \quad E^0 = +0.41\,\text{V vs. SHE} \tag{2}$$

$$\text{Overall}: \ BH_4^- + 2O_2 \rightarrow BO_2^- + 2H_2O, \quad E^0_{\text{cell}} = 1.64\,\text{V} \tag{3}$$

Borohydride is chemically stable in alkaline aqueous solution. It is easily stored, transported, refilled, and handled. Moreover, there is not catalyst poisoning for anode catalyst and less crossover problem in DBFC compared to direct methanol fuel cell (DMFC), which is one of the hottest research directions in direct liquid fuel cells. Besides, as shown in reaction (3) above, DBFC has a theoretical voltage of 1.64 V, which is much higher than other fuel cells using hydrogen and methanol as fuels with theoretical cell voltages of 1.24 V and 1.19 V, respectively.

Electrocatalyst is one of the key components in DBFC. In the past 10 years, different metals have been studied as anode catalysts: Pt [5–13], Au [1,5,6,14–17], Ag [18–21], Os [22,23], Ni [2,6,12,19,24–26], Pd, Cu [6], and kinds of hydrogen storage alloys [27–31]. Among of them, Pt and Ni are more attractive than other metals and proposed as anode catalysts for DBFC by many researchers. BH_4^- ion can take place strong electrochemical oxidation on Pt metal surface [5]. Wang et al. and co-workers thought that Ni, as a non-noble metal, also had visible electrocatalytic activity toward BH_4^- electrooxidation [25]. Employing Ni powder as anode catalyst, the DBFCs exhibited a good performance of 40 mW cm^{-2} [26].

As we know, bimetallic catalysts could achieve the higher activity and stability than monometallic ones. The bimetallic catalyst of PtNi/C has been widely investigated focusing on methanol electrooxidation and oxygen reduction reaction [32]. But researches focused on applying PtNi for borohydride electrooxidation were not widely investigated. For Ni, borohydride is a novel and special reagent, due to it can not only affect the activity of Pt, but also has activity toward the electrooxidation itself. Gyenge et al. [8] indicated that PtNi(1:1)/C was more active than Pt/C as anode catalyst for DBFC. However, only one specific molar ratio (1:1) of the PtNi/C catalyst was evaluated, and the compositions and physical characterizations of the PtNi/C catalysts were rarely analyzed. Geng et

* Corresponding authors. Tel.: +86 451 86417853; fax: +86 451 86413707.
E-mail addresses: gao_yunzhihit@yahoo.com.cn (Y.-z. Gao), yingphit@hit.edu.cn (G.-p. Yin).

0378-7753/$ – see front matter © 2009 Elsevier B.V. All rights reserved.
doi:10.1016/j.jpowsour.2009.06.080

al. [12] investigated three molar ratios of the PtNi/C catalysts with low amount of Pt. The result showed that the $Ni_{37}Pt_3$/C was the most active catalyst for BH_4^- electrooxidation and the electrocatalytic activity of Ni/C was even higher than that of Pt/C, which was opposed to the result published by others. Considering the importance of non-noble Ni in the electrochemical oxidation for BH_4^- and the contrary results in different literatures, more detailed information about the effect of Ni on Pt for BH_4^- electrochemical oxidation is urgent to be clarified. Considering the puzzles above, we carried out our investigations.

In this paper, Pt–Ni alloy catalysts were prepared by the borohydride reduction method and the effect of Pt alloying with Ni on the electrocatalytic activity toward the BH_4^- oxidation was carefully investigated by using cyclic voltammetry (CV) and *i–t* curves. The X-ray diffraction (XRD), energy dispersive analysis of X-ray (EDAX), and X-ray photoelectron spectroscopy (XPS) were also employed to characterize the chemical properties of Pt and Ni in alloy catalysts. The reasons for the electrocatalytic activity improvement of the alloy catalysts were analyzed.

2. Experimental

2.1. Preparation of catalysts

Pt/C, PtNi(7:3)/C, PtNi(5:5)/C, PtNi(3:7)/C, and Ni/C were prepared by the borohydride reduction method, with the same theoretical metal loading of 20 wt.%. The details are as follows: Carbon black powder (Vulcan XC-72, Cabot Inc.) was used as a support for the catalyst. $H_2PtCl_6{\cdot}6H_2O$ and $NiCl_2$ were used as precursors. The carbon black was ultrasonically dispersed in a solution of ultrapure water and isopropyl alcohol for 2 h. The precursors were added to the ink and then mixed thoroughly for another 2 h. The pH value of the ink was adjusted by a NaOH solution to 7 and then raised the temperature to 80 °C. A solution of 0.1 mol L^{-1} $NaBH_4$ was added dropwise into the ink, and the bath was stirred for 3 h. The mixtures were cooled, dried, and washed repeatedly with ultrapure water until no Cl^- ions exist. The catalyst powder was dried in a vacuum oven for 3 h at 80 °C and stored in a vacuum vessel.

2.2. Preparation of working electrode

Glassy carbon electrode with diameter of 3 mm polished with 0.05 μm alumina to a mirror-finish before each experiment was used as substrates for the carbon-supported catalysts. For electrode preparation, 5 μL of an ultrasonically redispersed catalyst suspension was pipetted onto the glassy carbon substrate. After the evaporation of the solvent at 60 °C, the deposited catalyst was covered with 1 μL of a dilute Nafion® solution. The resulting Nafion® film had sufficient strength to attach the Vulcan particles permanently to the glassy carbon electrode without producing significant film diffusion resistances.

2.3. Electrochemical measurements

Electrochemical measurements were carried out in a conventional three-electrode electrochemical cell. A glassy carbon electrode deposited with catalyst powder was used as the working electrode. A piece of Pt foil (1 cm^2) was used as the counter one. The Hg/HgO electrode (MOE) and standard hydrogen electrode (SHE) were used as the reference electrodes in electrocatalytic activity and electrochemical active surface area measurements, respectively. All chemicals used were of analytical grade. All the solutions were prepared with ultrapure water (MilliQ, Millipore) and purged with ultrapure argon gas. All electrochemical experiments were performed using a CHI630A electrochemical analysis instrument (CH instruments, Inc). Rotating disc electrode (RDE) experiments were carried out by using a glassy carbon disc electrode (3 mm diameter) coupled with the RRDE System (EG&G, Model 636). The electrocatalytic activity measurement (CVs and *i–t*) and electrochemical active surface area measurement (CVs) were recorded at rotating rates of 3000 rpm and 0 rpm, respectively. The scan rate of CVs was 0.1 V s^{-1}. CV curves were plotted at a potential range from −1.0 V to +0.4 V for electrocatalytic activity measurement in a solution of 6.0 mol L^{-1} NaOH containing 0.1 mol L^{-1} $NaBH_4$ and from 0.05 V to 1.2 V for electrochemical active surface area measurement in a solution of 0.5 mol L^{-1} H_2SO_4. The amperometric *i–t* test was carried out at −0.6 V for 400 s. All experiments were conducted at 25 ± 1 °C.

2.4. Physical characterization

The catalysts were characterized with X-ray diffraction (XRD, Japan D/max-rB diffractometer using a Cu Kα X-ray source operating at 45 kV and 100 mA). The metal loading of the catalysts were analyzed through energy dispersive analysis of X-ray (EDAX, attached to SEM system, Hitachi S4700).

X-ray photoelectron spectroscopy (XPS) analysis was performed to determine the chemical state of Pt and Ni with a Physical Electronics PHI model 5700 instrument. The Al X-ray source operated at 250 W. The sample to analyzer takeoff angle was 45°. Survey spectra were collected at pass energy (PE) of 187.85 eV over a binding energy range from 0 eV to 1300 eV. High binding energy resolution Multiplex data for the individual elements were collected at a PE of 29.55 eV. During all XPS experiments, the pressure inside the vacuum system was maintained at 1×10^{-9} Pa. Before analysis above, all the samples were dried under vacuum at 80 °C overnight.

3. Results and discussion

3.1. Electrocatalytic activity

The cyclic voltammetric (CV) curves of $NaBH_4$ electrooxidation on the PtNi/C catalysts with different molar ratios in an alkaline media are depicted in Fig. 1. By aid of RDE, the influence of concentration diffusion of fuel was markedly reduced and the reproducibility of the results was excellent. It can be seen clearly that there are remarkable oxidation peaks in CVs of pure Pt/C and Ni/C (insert part in Fig. 1), which confirms the conclusion that both Pt and Ni metals have electrocatalytic activities for BH_4^- electrooxidation [5,6,25]. However, the electrocatalytic activity of Ni/C was much lower than that of Pt/C. This result is different from the conclusions of the reference [12]. The different synthetic methods may be one of the reasons.

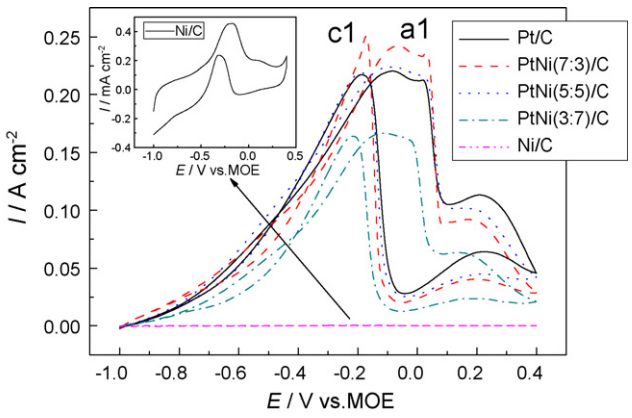

Fig. 1. CV curves of $NaBH_4$ electrooxidation on PtNi/C catalysts with different molar ratios. Scan rate: 0.1 V s^{-1}; electrolyte solution: 0.1 mol L^{-1} $NaBH_4$ + 6 mol L^{-1} NaOH; rotating rate: 3000 rpm; temperature: 25 ± 1 °C.

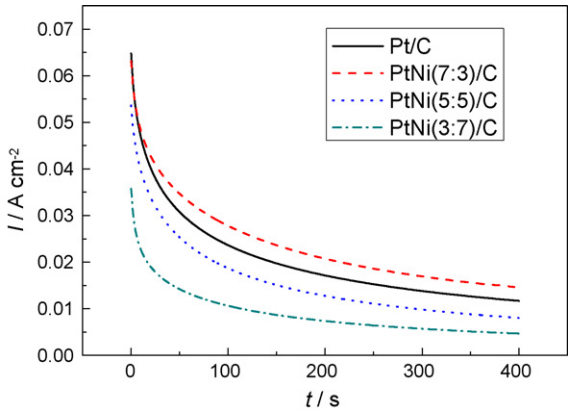

Fig. 2. The *i*–*t* curves of $NaBH_4$ on PtNi/C catalysts with different molar ratios at −0.6 V vs. MOE. Electrolyte solution: 0.1 mol L^{-1} $NaBH_4$ + 6 mol L^{-1} NaOH; rotating rate: 3000 rpm; temperature: 25 ± 1 °C.

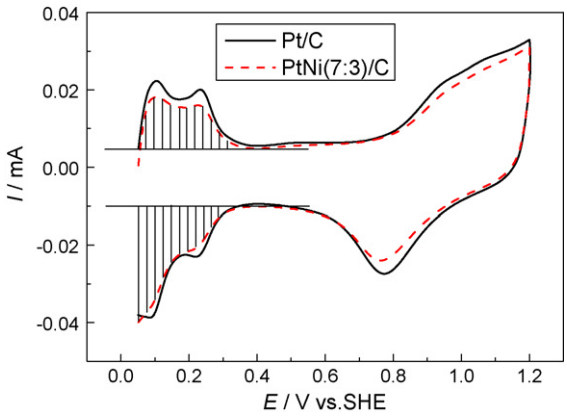

Fig. 3. CV curves of the Pt/C and PtNi(7:3)/C catalysts in 0.5 mol L^{-1} H_2SO_4. Scan rate: 0.1 V s^{-1}; temperature: 25 ± 1 °C.

In the positive scanning direction in CVs, it can be seen that a wide oxidation peak a1 appears between −0.6 V and +0.1 V, which is attributed to the electrooxidation of the intermediate of BH_4^- hydrolysis reaction, i.e. BH_3OH^-. The peak c1 in the negative scanning direction is also due to BH_3OH^- electrooxidation, but on the partially oxidized Pt surface [5]. The current density of peak a1 can be employed to evaluate the electrocatalytic activity of the catalysts. Among PtNi/C catalysts with different molar ratios, PtNi(7:3)/C presented the highest peak current density (0.242 A cm^{-2}), which was 10% higher than that of Pt/C catalyst (0.220 A cm^{-2}). Furthermore, the onset peak potential of PtNi(7:3)/C shown in Fig. 1 is more negative than that of other catalysts. The more negative of the onset peak potential is, the higher performance of fuel cell is.

The steady-state current densities at a constant potential were used to compare the performances of PtNi/C catalysts with different molar ratios for BH_4^- electrooxidation. Fig. 2 shows *i*–*t* curves measured in an Ar-saturated solution of 0.1 mol L^{-1} $NaBH_4$ + 6.0 mol L^{-1} NaOH at 25 ± 1 °C. A potential of −0.6 V was employed when measuring *i*–*t* curves.

As shown in Fig. 2, the initial current densities of Pt/C and PtNi(7:3)/C are similar. The current decay over time is parabolic and reached an apparent steady state within 400 s. The current decay rate over time on Pt/C catalyst is faster than that of PtNi(7:3)/C. The final current densities of Pt/C, PtNi(7:3)/C, PtNi(5:5)/C and PtNi(3:7)/C are 11.7, 14.59, 8.04 and 4.69 mA cm^{-2}, respectively. The final current density of PtNi(7:3)/C is the highest one (24.7% higher than that of Pt/C) at the same potential(−0.6 V), i.e. the activity of the PtNi(7:3)/C is the best. This result is consistent with that of CV measurement.

For the sake of analyzing the effect of Ni on Pt, the final current density of PtNi(7:3)/C, PtNi(5:5)/C and PtNi(3:7)/C are normalized with respect to the amount of Pt in Pt/C, which is defined as I_{pt}. And then, the I_{pt} of Pt/C, PtNi(7:3)/C, PtNi(5:5)/C and PtNi(3:7)/C are 11.7 mA cm^{-2}, 16.47 mA cm^{-2}, 10.46 mA cm^{-2} and 8.0 mA cm^{-2}, respectively. The I_{pt} of Pt/C and PtNi(5:5)/C are closed. The I_{pt} of PtNi(7:3)/C is 40.7% higher than that of Pt/C. But the I_{pt} of PtNi(3:7)/C is lower than that of Pt/C. Thus, we consider that a proper content of Ni can enhance the I_{pt} of PtNi/C catalysts due to the electronic structure change of Pt. But if too many Ni are added, several Pt surface would be covered by Ni or its oxides/hydroxides, which would result in a lower activity of catalyst.

3.2. Effect of Ni on the performance of Pt/C catalyst

It is well known that larger electrochemical active surface area (S_{EAS}) would be one of the reasons of higher activity of the Pt/C catalyst. To analyze the effect of Ni on the S_{EAS} of the Pt/C catalyst, the S_{EAS} of the Pt/C and PtNi(7:3)/C catalysts were measured comparatively.

S_{EAS} of the catalyst can be calculated from the charge transfer (Q_H, mC mg^{-1} Pt) for the hydrogen adsorption [33] or desorption [32] in the hydrogen region (0.05–0.4 V, corresponding to the hatched parts in Fig. 3.) of cyclic voltammograms. We choose the average of them here in order to reduce the experimental error. The constant for S_{EAS} calculation is 0.21 mC cm^{-2} [33] and then the value of the S_{EAS} is obtained from: $S_{EAS} = Q_H/0.21$.

Fig. 3 shows the CVs of the Pt/C and PtNi(7:3)/C measured in 0.5 mol L^{-1} H_2SO_4 aqueous solution at a scan rate of 0.1 V s^{-1}. By calculation, the S_{EAS} of Pt/C and PtNi(7:3)/C are 17.26 m^2 g^{-1} Pt and 16.55 m^2 g^{-1} Pt, respectively. The result indicates that the two catalysts have the similar S_{EAS}. On the other hand, the theoretical Pt metal loading of PtNi(7:3)/C is only 88.6% that of Pt/C. PtNi(7:3)/C with less S_{EAS}, however, has a higher electrocatalytic activity toward BH_4^- electrooxidation due to the addition of Ni. Hence, the factor of electrochemical active area cannot be the key reason for the electrocatalytic activity improvement of the PtNi(7:3)/C catalyst.

The X-ray diffraction (XRD) patterns of the Pt/C and PtNi(7:3)/C catalysts as shown in Fig. 4 clearly demonstrate the characteristic peaks of the Pt fcc structure, but no characteristic peaks of Ni or its oxides/hydroxides are detected in PtNi(7:3)/C catalyst. This could be the result of alloy formation between Pt and Ni since platinum is known to be alloyed well with Ni [34]. Besides, an obvious angle shift of the Pt peak occurs on the PtNi(7:3)/C. As shown in Fig. 4, the 2θ of the Pt(1 1 1) peak for Pt/C and PtNi(7:3)/C are 39.92

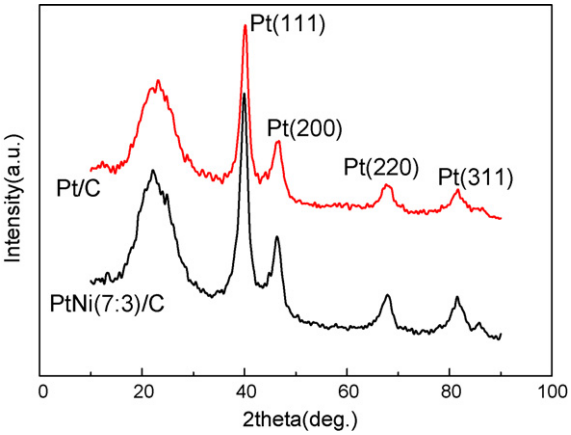

Fig. 4. X-ray diffraction patterns of the Pt/C and PtNi(7:3)/C catalysts.

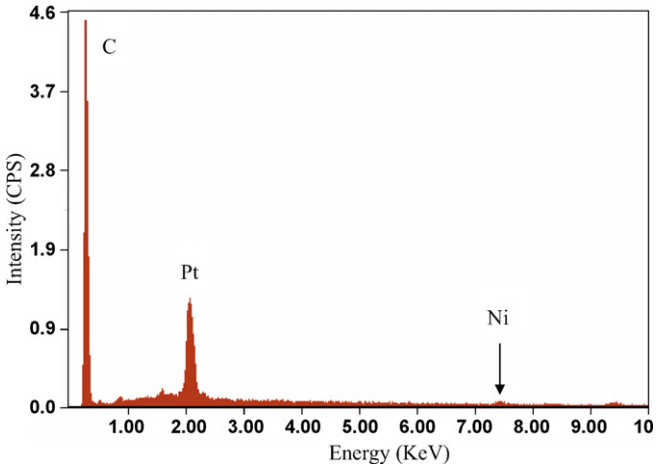

Fig. 5. EDAX pattern of the PtNi(7:3)/C catalyst.

and 40.17, respectively. The same trend is also shown in 2θ of the Pt(2 0 0) peaks [46.32 (Pt/C), 46.76 (PtNi(7:3)/C)]. The higher angle shifts of the Pt peaks also indicate an alloy formation between Pt and Ni, which is the evidence that the PtNi alloy nanoparticles are successfully deposited on carbon black powder (Vulcan XC-72). The hydrogen adsorption and desorption on the surface of Pt would be weakened by alloy formation between Pt and Ni [35], which maybe one reason of that the S_{EAS} of PtNi(7:3)/C becomes smaller than that of Pt/C (Fig. 3).

On the other hand, the angle shifts of the Pt peaks are not very high, i.e. 0.25 and 0.54 for Pt(1 1 1) and Pt(2 0 0) peaks, respectively. Maybe alloy formation is not the only effect approach of Ni on the activity of Pt.

The average particle sizes of Pt/C and PtNi(7:3)/C catalysts from XRD patterns are about 4.9 nm and 5.0 nm, respectively, as calculated using the Debye–Scherrer Formula (Eq. (4)) [35], where the d is average particle size, k is a constant of 0.9, λ is the wavelength of X-ray, θ is the angle of (2 2 0) peak, and $\beta_{1/2}$ is the peak width at half height.

$$d = \frac{k\lambda}{\beta_{1/2}\cos\theta} \quad (4)$$

The average particle sizes between Pt/C and PtNi(7:3)/C catalysts are almost similar, indicating that the particle size effect of catalyst cannot account for the higher electrocatalytic activity of PtNi(7:3)/C in comparison to Pt/C.

The result of the EDAX pattern of the PtNi(7:3)/C (Fig. 5) presents the existence of Pt and Ni. It shows that the total metal loading of PtNi(7:3)/C is 23.6 wt.% and the molar ratio of Pt and Ni is 7:2.4. Both the measured values agree mainly with the expected theoretical ones, i.e. 20 wt.% and 7:3, respectively. The values of metal loading and molar ratio of Pt and Ni were obtained automatically by EDAX attached to SEM system, but not calculated artificially.

To further investigate the chemical properties of PtNi nanoparticles, XPS analyses were performed. The spectra of Pt 4f (Fig. 6) and Ni 2p (Fig. 7) were mutiplely fitted with a mixed Gaussian–Lorentzian line shape. Table 1 shows the XPS data and the possible chemical states of Pt and Ni in Pt/C and PtNi(7:3)/C catalysts. No XPS peaks of chloride were found, showing that the chloride ions were completely removed during washing.

As shown in Table 1, the content of Pt(II) in PtNi(7:3)/C is almost the same as that in Pt/C, but the content of Pt(0) in PtNi(7:3)/C (69.0%) is 10% more than that in Pt/C (59.8%), at the same time, the content of Pt(IV) in PtNi(7:3)/C (12.1%) is 10% less than that in Pt/C (23.7%). Considering the content of Pt in total metal for PtNi(7:3)/C (88.6%), the content of Pt(0) in total metal for PtNi(7:3)/C is 61.1%

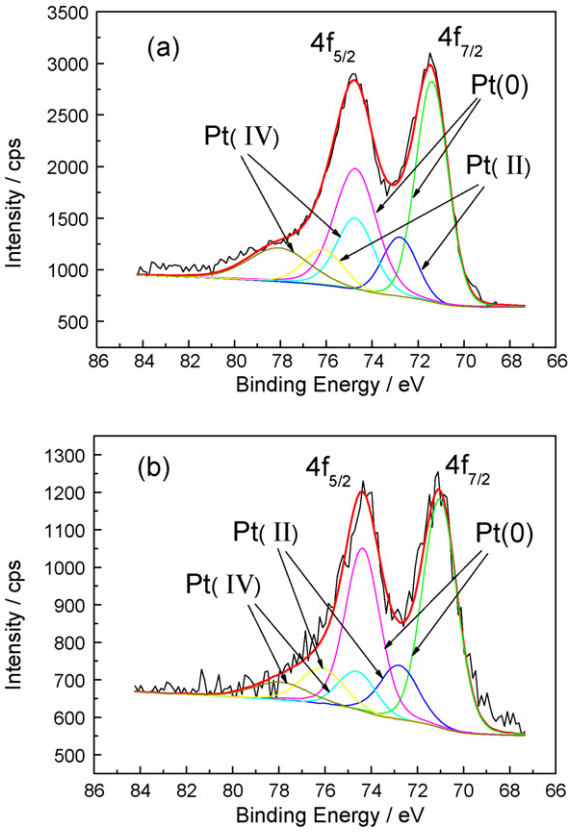

Fig. 6. Pt 4f XPS spectra of the Pt/C (a) and PtNi(7:3)/C (b) catalysts.

which is also bigger than that in Pt/C (59.8%). As a result, the higher content of Pt(0) could be one of the reasons for a catalyst to generate higher electrocatalytic activity. The presence of Ni oxides, such as $Ni(OH)_2$ and NiOOH, could result in the increase of the Pt(0) and the decrease of Pt(IV) due to the electronic effect of Ni on Pt.

In contrast, the Ni 2p spectrum shows a complex structure with intense satellite signals of high binding energy adjacent to the main peaks, which may be ascribed to a multielectron excitation (shake-up peaks) (Fig. 7.). Curve fitting of the Ni 2p signal gives different nickel species. Considering the shake-up peaks, the Ni $2p_{3/2}$ XPS peaks at the binding energies of 855.8 eV, and 857.1 eV are ascribed to $Ni(OH)_2$ and NiOOH, respectively [34].

Furthermore, with reference to Pt/C, the Pt 4f XPS spectrum of PtNi(7:3)/C experiences peak shifts −0.4 eV both for Pt $4f_{7/2}$ (71.1 eV for Pt/C) and Pt $4f_{5/2}$ (74.4 eV), which indicates an electronic

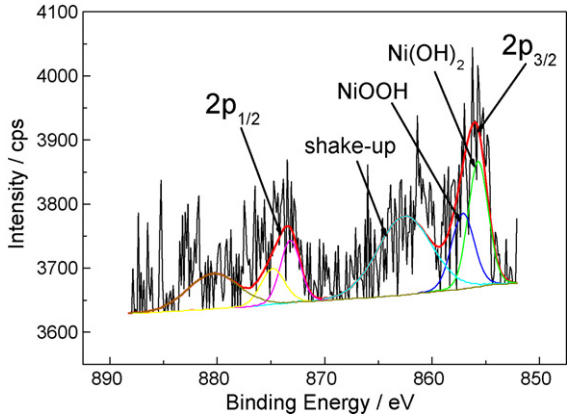

Fig. 7. Ni 2p XPS spectra of the PtNi(7:3)/C catalyst.

Table 1
XPS data and the possible chemical states of Pt and Ni in the Pt/C and PtNi(7:3)/C catalysts.

Sample	Pt(0)	Pt(II)	Pt(IV)	Ni ($Ni(OH)_2$)	Ni (NiOOH)
Pt/C	71.39[a], 74.72	72.79, 76.12	74.73, 78.06		
	59.8%[b]	16.5%	23.7%		
PtNi(7:3)/C	71.03, 74.37	72.80, 76.13	74.61, 77.94	855.7, 873.2	857.1, 874.8
	69.0%	18.9%	12.1%	59.4%	40.6%

[a] B.E. in eV.
[b] Content percent.

state change of Pt when it was alloyed with Ni. Most likely, Ni(0) replaces Pt atom and occupies the platinum lattice, which cannot be captured by XRD, and the metallic grains are intermixed with amorphous Ni hydroxides, such as $Ni(OH)_2$ and NiOOH revealed in the XPS spectra. Peaks due to the hydroxides or oxides of Ni are not also observed by XRD because of their amorphous nature [36]. Moreover, the Ni hydroxide layer has some other favorable properties, such as proton and electronic conductivity.

4. Conclusions

Carbon-supported Pt, Ni, and PtNi alloy catalysts were prepared by borohydride reduction method. The CVs results show that both Pt and Ni have obvious electrocatalytic activity to BH_4^- oxidation. Among PtNi/C catalysts with different molar ratios, PtNi(7:3)/C presents the highest electrocatalytic activity. The addition of Ni to Pt/C results in the improvement of the electrocatalytic activity. PtNi alloy formation induces the co-catalytic effect of Ni on the BH_4^- electrooxidation. The higher content of Pt(0) in PtNi(7:3)/C could be another reason for its higher electrocatalytic activity compared to Pt/C.

References

[1] S.C. Amendola, P. Onnerud, T.M. Kelly, P.J. Petillo, S.L. Sharp-Goldman, M. Binder, J. Power Sources 84 (1999) 130.
[2] Z.P. Li, B.H. Liu, K. Arai, S. Suda, J. Electrochem. Soc. 150 (2003) A868.
[3] M.E. Indig, R.N. Snyder, J. Electrochem. Soc. 109 (1962) 1104.
[4] R. Jasinski, Electrochem. Technol. 3 (1965) 40.
[5] E. Gyenge, Electrochim. Acta 49 (2004) 965.
[6] B.H. Liu, Z.P. Li, S. Suda, Electrochim. Acta 49 (2004) 3097.
[7] J.H. Kim, H.S. Kim, Y.M. Kang, M.S. Song, S. Rajendran, S.C. Han, D.H. Jung, J.Y. Lee, J. Electrochem. Soc. 151 (2004) A1039.
[8] E. Gyenge, M. Atwan, D. Northwood, J. Electrochem. Soc. 153 (2006) A150.
[9] K. Deshmukh, K.S.V. Santhanam, J. Power Sources 159 (2006) 1084.
[10] A. Verma, S. Basu, J. Power Sources 174 (2007) 180.
[11] J.I. Martins, M.C. Nunes, R. Koch, L. Martins, M. Bazzaoui, Electrochim. Acta 52 (2007) 6443.
[12] X.Y. Geng, H.M. Zhang, W. Ye, Y.W. Ma, H.X. Zhong, J. Power Sources 185 (2008) 627.
[13] J.I. Martins, M.C. Nunes, J. Power Sources 175 (2008) 244.
[14] M.H. Atwan, C.L.B. Macdonald, D.O. Northwood, E.L. Gyenge, J. Power Sources 158 (2006) 36.
[15] C. Ponce-de-León, D.V. Bavykin, F.C. Walsh, Electrochem. Commun. 8 (2006) 1655.
[16] F.A. Coowar, G. Vitins, G.O. Mepsted, S.C. Waring, J.A. Horsfall, J. Power Sources 175 (2008) 317.
[17] M. Chatenet, M.B. Molina-Concha, J.P. Diard, Electrochim. Acta 54 (2009) 1687.
[18] E. SanlI, H. Çelikkan, U.B. Zühtü, M.L. Aksu, Int. J. Hydrogen Energy 31 (2006) 1920.
[19] R.X. Feng, H. Dong, Y.L. Cao, X.P. Ai, H.X. Yang, Int. J. Hydrogen Energy 32 (2007) 4544.
[20] M.H. Atwan, D.O. Northwood, E.L. Gyenge, Int. J. Hydrogen Energy 32 (2007) 3116.
[21] E. Sanli, B.Z. Uysal, M.L. Aksu, Int. J. Hydrogen Energy 33 (2008) 2097.
[22] M.H. Atwan, D.O. Northwood, E.L. Gyenge, Int. J. Hydrogen Energy 30 (2005) 1323.
[23] V.W.S. Lam, E.L. Gyenge, J. Electrochem. Soc. 155 (2008) B1155.
[24] B.H. Liu, Z.P. Li, S. Suda, J. Electrochem. Soc. 150 (2003) A398.
[25] G.J. Wang, G.P. Yin, Y.Z. Gao, ECS Meeting Abstracts 701 (2007) 183.
[26] G.J. Wang, Y.Z. Gao, Z.B. Wang, K.D. Cai, J. Zhang, G.P. Yin, J. Chem. Eng. Chin. Univ. 22 (2008) 666.
[27] L.B. Wang, C.A. Ma, X.B. Mao, J.F. Sheng, F.Z. Bai, F. Tang, Electrochem. Commun. 7 (2005) 1477.
[28] L.B. Wang, C.A. Ma, Y.M. Sun, S. Suda, J. Alloys Compd. 391 (2005) 318.
[29] L.B. Wang, C.A. Ma, X.B. Mao, J. Alloys Compd. 397 (2005) 313.
[30] B.H. Liu, S. Suda, J. Alloys Compd. 454 (2008) 280.
[31] Z.Z. Yang, L.B. Wang, Y.F. Gao, X.B. Mao, C.A. Ma, J. Power Sources 184 (2008) 260.
[32] E. Antolini, J.R.C. Salgado, A.M. dos Santos, E.R. Gonzalez, Electrochem. Solid State 8 (2005) A226.
[33] V.A. Sethuramana, J.W. Weidnera, A.T. Haugb, M. Pembertonb, L.V. Protsailo, Electrochim. Acta (2009), doi:10.1016/j.electacta.2009.04.062.
[34] G. Casella, M.R. Guascito, M.G. Sannazzaro, J. Electroanal. Chem. 462 (1999) 202.
[35] H. Yang, C. Coutanceau, J.-M. Leĭger, N. Alonso-Vante, C. Lamy, J. Electroanal. Chem. 576 (2005) 305.
[36] T.C. Devaraj, W.X. Chen, J.Y. Lee, J. Mater. Chem. 13 (2003) 2555.